EXPLORING PRACTICAL APPROACHES TO SOUND ABSORPTION MEASUREMENT: VALIDATING A REPURPOSED SPACE AS A SMALL-SCALE REVERBERATION ROOM

David Bosonin[1], Lukas Gölles[2], Louena Shtrepi[1], Milena Stavric[3], Franz Zotter[2]
[1] *Politecnico di Torino, Corso Duca degli Abruzzi 24, 10129 Torino, Italy*
[2] *University of Music and Performing Arts, Institute of Electronic Music and Acoustics, Inffeldgasse 10/3, 8010 Graz, Austria*
[3] *Graz University of Technology, Rechbauerstrasse 12, 8010 Graz, Austria*

Abstract

While normal-incidence absorption can be measured with a simple impedance tube (ISO 10534-2), its random-incidence counterpart (ISO 354) assumes a level of infrastructure most research laboratories simply don't have. This paper first compares these two standardized methods with several non-standardized alternatives, weighing their accuracy, practicality, and cost in a summary table intended as a practical guide for selecting the one best suited to specific needs and budget. It then addresses the specific case of small-scale reverberation rooms, evaluating a small, unmodified bathroom as a low-cost alternative to a dedicated reverberation chamber. The validity of this approach is assessed by comparing the absorption coefficients obtained in the adapted room with those measured in an impedance tube, across three sample configurations of increasing exposed area. The results show that compatibility between the two methods depends on two independent conditions: measuring above the room's Schroeder frequency, and using a sufficiently large sample area, neither being sufficient on its own. These findings provide a practical guideline for researchers with limited resources seeking to validate small-scale reverberation room measurements in non-dedicated spaces.

Keywords: *acoustic characterization, absorption measurements, small-scale reverberation room*

Corresponding author: *davidbosonin@gmail.com*

1. Introduction

In the design or refurbishment of acoustic environments, a key aspect is the choice of sound-absorbing materials, classified primarily according to their sound absorption coefficient α. Defined as "the fraction of incident sound energy absorbed by the surface or medium" [1], it is formally measured using two standardized approaches, the impedance tube method (ISO 10534-2) [2] and the reverberation room method (ISO 354) [3]. Alongside these, several non-standardized methods have been validated in the literature, allowing researchers and manufacturers to carry out reliable measurements without the costly infrastructure required by the standards. The first part of this paper reviews all of these methods, standardized or not, comparing them in a summary table conceived as a practical guide to help navigate the choice of the method best suited to one's own needs and budget. The second part of the study takes a more targeted approach, investigating the repurposing of a small bathroom, available in almost every research facility, as a miniature reverberation room, exploiting its typically highly reverberant nature. The absorption coefficients of a melamine resin foam sample measured here are compared with those obtained in the impedance tube to assess the validity of this approach. This practice fills a gap in the literature, where proposed small-scale reverberation rooms (SSRRs) have almost always required building new dedicated boxes or spaces, an option not always feasible for laboratories with limited budgets.
This study therefore examines whether reusing an existing space can serve as a viable, low-cost alternative to standard methods, without excessively compromising the validity of the results. Such an approach would

also allow comparative testing between complex designs at an early development stage, for research or educational purposes.

2. Overview and Comparison of Sound Absorption Measurement Methods

Determining the sound absorption coefficient requires reconciling competing objectives, specifically maximizing the physical representativeness of the measurement while maintaining acceptable levels of cost and experimental practicality. The techniques discussed herein reflect different compromises between these factors, with each method developed to address specific limitations of the preceding one.

2.1. Full Scale Reverberation Room (ISO 354)

The starting point of this review is the full-scale reverberation room (FSRR) method [3], currently under revision to address some of the limitations still present in its current iteration [4], [5]. It is the principal normative reference, being the only one whose measurement condition faithfully reproduces the diffuse field, where sound strikes the specimen uniformly from all directions and the sound intensity is uniform throughout the space, thus allowing the random-incidence absorption coefficient to be calculated [3]. Such a condition corresponds to the physical reference model assumed in design practice for the real-world use of sound-absorbing materials [6]. Conversely, in situ measurements, which we will discuss later, yield a site-specific result, accounting for the particular conditions of that installation, rather than a general and transferable descriptor of the material [3], [7]. This accuracy comes at the price of very large room volumes and specimen sizes, resulting in high costs and limited access for many laboratories [8], [9], prompting research to turn toward more accessible, yet still accurate, solutions.

2.2. Small Scale Reverberation Room

Several studies have applied the principles of ISO 354 to SSRRs, built to the same diffuse-field logic as FSRRs, but at a reduced scale, typically a few cubic meters instead of the hundreds required by the latter [8], [10], [11], [12], [13]. Their reduced size allows savings in both cost and material [8], [13], while also enabling the measurement of three-dimensional objects of various sizes [8], [10], [11], [12]. The price is a rise in the room's Schroeder frequency, the limit below which the field ceases to be diffuse and organizes itself into discrete modes, invalidating Sabine's equation, on which ISO 354 is based [3], [14]. New solutions have recently emerged, addressing this unreliability at low frequencies: Kierzkowski [12] extrapolates data measured at higher frequencies to estimate the lower ones, while Ćurović [9] couples the measured modal decay with an eigenvalue-based FEM model.

2.3. Impedance Tube (ISO 10534-2)

A radically different approach is the impedance tube method, which, rather than attempting to reproduce the complexity of the diffuse field, eliminates it altogether [2]. The measurement is carried out inside a rigid and sealed duct, with a sound source at one end and the specimen at the other. In the most common configuration, two microphones positioned in between decompose the generated wave, plane by construction, into an incident and a reflected component [2], [15], [16]. The measurement yields the normal-incidence absorption coefficient, that is, relative to a wave striking the specimen perpendicularly to its surface [2]. The trade-off for this experimental simplicity, however, is representativeness, since perpendicular incidence rarely occurs in real environments, where sound reaches surfaces from every direction [12].

2.4. In Situ Methods

To address situations where a specimen cannot be moved to a dedicated laboratory, a large number of in situ techniques have been developed, measuring the material directly on site [17]. These range from single-point probes to spatial microphone arrays.

2.4.1. Point-Probe Techniques

Point-probe techniques divide into methods based on temporal separation, and methods based on direct impedance measurement. The first separates the reflected sound from the direct sound in time, then derives the absorption coefficient through spectral analysis [18], [19]. Specifically, Garai [18] uses a time window, while Mommertz [19] subtracts a free-field reference response from the in situ measurement, also enabling measurement at oblique incidence. The second family employs a different technique, measuring the acoustic impedance near the surface of the sample: Allard [20] obtains it from the pressure gradient between two microphones, while Lanoye [21] uses a Microflown probe, which combines a microphone and particle-velocity sensor. Both methods, however, share two fundamental limitations. The first concerns the field itself, since near the surface the emitted wave is still spherical rather than plane, yet the formula describing its reflection requires the impedance one is trying to measure, a problem solvable only through successive approximations [17], [20]. The second concerns the material, assumed to be locally reacting, meaning it responds point by point without lateral sound propagation. This approximation is valid for many common absorbing materials, but not all [17].

2.4.2. Spatial Array Techniques

The two previous limitations are not a technical detail, but structural constraints. Both can be avoided by working over an entire plane rather than a single point, removing the plane-wave assumption and the need for a locally reacting material. Tamura [22], [23] does so by measuring the pressure over two entire planes and decomposing it using a spatial Fourier transform, thereby obtaining the incident and reflected components at every angle of incidence. What suffers, in this case, is practicality, since a single microphone needs to be moved across an extremely large number of positions, and the transform itself presupposes periodicity, requiring large surfaces in order to limit the resulting error [24]. Hald [24] later eases this burden by using a double-layer microphone array that acquires everything in a single measurement and by applying SONAH holography, instead of the Fourier transform, in order to reconstruct the field without assuming periodicity.

2.5. Sound Field Synthesis

Dupont [25] brings the journey to its most recent turning point, upending the underlying logic seen so far. Rather than measuring an imperfect field and then correcting it, he builds a perfect field beforehand, within which the measurement is then carried out. A virtual array, created by moving a loudspeaker across multiple positions, synthesizes a plane wave on the specimen's surface at each desired angle of incidence, and the absorption coefficient is then derived from the transfer function between two microphones placed near the surface [25]. Repeating the measurement at different angles and combining the results with Paris' formula [26] yields the diffuse-field coefficient. The strong direct component near the surface also removes edge diffraction and noise, so the coefficient never exceeds unity, an anomaly that has long affected the reverberation room technique [25], [27].

2.6. Summary and Conclusions

The trade-off we started from, representativeness or practicality, is never resolved once and for all; it simply resurfaces in a different form every time. Each method discussed here confronts it by choosing what to sacrifice: the reverberation room gives up accessibility, the impedance tube gives up representativeness, and in situ techniques give up procedural simplicity. There is no definitive method, only a different compromise for every need. The table below (Table 1) is designed to help the reader navigate this variety, guiding their choice toward the method best suited to their own requirements.

3. Theoretical Background

Sabine's equation. As introduced in Section 2, the reverberation room method assumes a perfectly diffuse sound field, with acoustic energy distributed homogeneously and isotropically in space [1], [3]. Under this assumption, sound decay follows Sabine's equation [28]:

$$T = 0.161\frac{V}{A} \tag{1}$$

which, combined with the equivalent absorption area equation [28]

$$A = \sum_i \alpha_i S_i, \tag{2}$$

allows the random-incidence absorption coefficient to be derived as follows [3]:

$$\alpha_S = \frac{0.161V}{S}\left(\frac{1}{T_2} - \frac{1}{T_1}\right) \tag{3}$$

where T_1 and T_2 are the reverberation times measured respectively without and with the specimen, and S is the specimen area.

Reverberation time estimation. The reverberation time T underlying Sabine's equation is defined as the time required for the sound level in a room to decay by 60 dB after source emission has stopped [29]. In practice, achieving a sufficient SNR for this is very difficult, so T30 (extrapolated from a −5 to −35 dB decay segment) was used throughout this study, following the ISO/CD 354:2019 draft revision [5].

The Schroeder frequency. The validity of the diffuse field hypothesis depends on the modal density of the room and finds its conventional limit at the Schroeder frequency [14]:

Table 1: Comparison of sound absorption measurement methods

Property	FSRR [3], [4], [5]	SSRR [8], [9], [10], [11], [12], [13]	Impedance Tube [2]	Point-Probe: time-domain [18], [19]	Point-Probe: direct impedance [20], [21]	Spatial Array [22], [23], [24]	Sound Field Synthesis [25]
Absorption coefficient type	Random incidence	Random incidence	Normal incidence	Normal [18] and oblique incidence [19]	Normal [20] and oblique incidence [21]	Normal and oblique incidence	Normal and oblique incidence; random incidence via Paris' formula
Required facility	Reverberation room, ≥ 150 m^3 (CD 2019: 190-350 m^3)	Small-scale reverberation room (1-10 m^3)	Laboratory	None (portable setup)	None (portable setup)*	Anechoic room (SFT) [23] to portable setup (SONAH) [24]	Semi-anechoic chamber
In situ capable?	No	No	No	Yes	Yes (unverified for [21])	Yes	No
Sample requirements	10–12 m^2 (plane); 1–12 m^2 ΔA_{abs} (discrete)	0.2–1.5 m^2	Few cm^2; flat and homogeneous	> 4 m^2; flat	0.02–1.4 m^2 (normal) to ≥ 2.16 m^2 (oblique); locally-reacting surface	≥ 4 m^2 (SFT) to 0.1–4.3 m^2 (SONAH, homogeneous)	2.25 m^2 (1 m^2 if >300 Hz); homogeneous and isotropic
Suitable for 3D objects?	Yes	Yes (footprint ≤ 30% of floor area) [11]	No	No	No	No	No
Reliable frequency range	100–5000 Hz	400–5000 Hz (porous); from 1000 Hz (thin rigid) [8]	Set by tube diameter and mic spacing; 100–5000 Hz via two tubes [8]	> 300 Hz, upper limit set by sample-surface roughness [18]; 250 Hz–8000 Hz [19]	Up to 2000 Hz (≥500 Hz for weak abs.) [20]; 150–3000 Hz; up to 6400 Hz [21]**	500–3000 Hz [23]; 200–5000 Hz [24]	100–4000 Hz (declared); 150–3000 Hz (validated)
Cost & complexity	Very high: costly dedicated room [8], large samples	Moderate: cheaper construction than FSRR; less material and waste	Low: minimal material, no dedicated room	Low: portable, low-cost instrumentation	Low (two-microphone); moderate (PU probe, calibration)	High: anechoic room, mechanical scanning apparatus [23]; array hardware cost [24]	High: semi-anechoic chamber, precision motorized stages

**Weakly-absorbing materials require a large/anechoic room [20]. **Extended range achieved via free-field calibration, at the cost of reduced accuracy at low frequencies [21].*

$$f_s = 2000\sqrt{\frac{T}{V}} \quad (4)$$

Below this threshold, resonant modes remain isolated, the diffuse field hypothesis no longer holds, and Sabine's equation loses validity [14]. Since f_s is inversely proportional to the square root of the volume, in small-volume rooms, like the one used within this study, it is considerably higher than that of an ISO 354-compliant chamber. As a result, below f_s the measured reverberation time no longer matches Sabine's prediction, and the values obtained cannot be considered reliable, a limitation widely reported in the literature for SSRRs [8], [9], [10], [12], [13].

Normal vs. random incidence coefficients. The normal-incidence absorption coefficient, provided by impedance tube measurements [2], describes the material's response to a wave striking perpendicular to its surface, while the random-incidence coefficient, provided by reverberation room measurements [3], represents the weighted average over all directions of incidence, according to the statistics of the diffuse field. The two are only theoretically related through Paris' formula:

$$\alpha_S = 2\int_0^{\frac{\pi}{2}} \alpha(\theta)\sin(\theta)\cos(\theta)d\theta \quad (5)$$

and are not expected to be numerically coincident even under ideal conditions [26]. A further source of divergence between the two stems from the finite area of the specimen. In reverberation room measurements, diffraction at the specimen's edges tends to overestimate α_S, especially at medium-high frequencies, occasionally leading to values exceeding unity [8], [25], [27].

4. Methodology

4.1. The Repurposed Room

To test whether an ordinary space can be repurposed as an SSRR, this study uses a small and unmodified bathroom rather than a purpose-built reverberation room, a solution replicable even by laboratories with limited resources. The room (Figure 2) has a volume of $V = 8.96\text{m}^3$, an irregular shape, and a height of 2.75 m. Inside it are a sink, a mirror, a light fixture, a small boiler, a radiator, and a paper towel dispenser, fixed elements that could not be removed during the measurements. The floor, as well as more than half of the wall surface, is tiled, while the remaining walls and the ceiling are plastered and painted; two walls are also interrupted by doors. Consistent with the principle of practicability in non-specialized environments, no additional diffusers were installed.

4.2. Measurements Procedures

4.2.1. Measurement in the Adapted SSRR

The material tested in both the SSRR and the impedance tube is melamine resin foam, in the form of rigid panels with dimensions $121.5 \times 54 \times 7.8$ cm. Each panel was mounted flush against the wall, exposing only one face to the room, so as to obtain the absorption coefficient of that single face, closer to the condition used in impedance tube measurements [2]. Three configurations were tested, using 1, 2, and 3 panels against the same wall, corresponding to exposed sample areas of 0.66, 1.31, and 1.97 m^2 respectively (Figure 1). This progression allowed the influence of sample area on the measured absorption coefficient to be assessed independently of other room parameters.

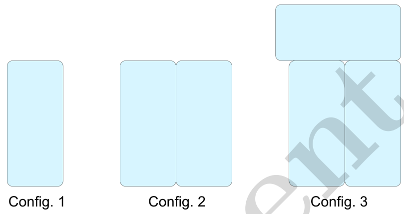

Figure 1: Layout of the 1-, 2-, and 3-panel configurations against the wall.

The measurement setup consisted of a Focusrite Scarlett 18i8 (Gen 2) audio interface, 3 Genelec 8020B loudspeakers, and 4 NTI Audio M4262 omnidirectional microphones, for a total of 12 source-microphone combinations, as required by ISO 354 [3]. Microphones and loudspeakers were positioned as far apart as possible, so as to capture as broad a portion of the sound field as possible (Figure 2), at least 30 cm from the walls, 50 cm from the ceiling and floor, 40 cm from each other, more than twice the critical distance, beyond which the source's direct field becomes negligible compared to the reverberant field [6], [29]. Loudspeakers were also oriented toward the room's corners to ensure uniform excitation of the room modes [4].

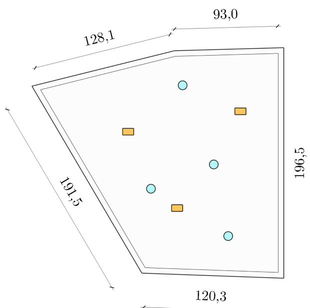

Figure 2: Floor plan of the room, showing the position of loudspeakers (orange) and microphones (light blue).

A custom Python script generated the sweeps and processed the reverberation times. The signal was a multi-sweep of three logarithmic sweeps in sequence, each lasting 10 s from 200 Hz to 8000 Hz, played through a different loudspeaker with a 2 s pause between sweeps. Reverberation time was calculated as T_{30}. For each configuration, 6 repeated measurements were taken within a short time interval, ensuring near-constant environmental conditions (approximately

24.3 °C and 50% relative humidity) between measurements.

4.2.2. Measurement with the Impedance Tube

Impedance tube measurements were carried out on the same material, using a custom-built tube with an internal diameter of 10 cm, a length of 62.5 cm, a microphone spacing of 5.5 cm, and a distance of 8.5 cm between the nearest microphone and the specimen surface. The sound source was a custom-built loudspeaker, excited with white noise lasting 5.8 s. The specimen had a thickness of 7.8 cm and was mounted with a rigid termination. A single measurement was carried out, with no repetitions. A custom Matlab script calculated the absorption coefficient from the transfer function between the two microphones [2]. Measurements were conducted at a temperature of approximately 27.5 °C and a relative humidity of 54%.

5. Results

The Schroeder frequency was computed from a single empty-room measurement taken immediately before testing the three configurations, within the same five-minute session, using the mean T_{30} in the 500-1000-2000 Hz bands ($T_{30} = 0.93$ s), yielding $f_s = 643.6$ Hz, used as the lower validity bound for the Sabine-based estimates reported below.

5.1. Effect of sample area on absorption coefficient

Figure 3 shows $\alpha_{SSRR(f)}$ for the three configurations, corresponding to exposed sample areas of 0.66, 1.31 and 1.97 m^2. Above f_s, α decreases systematically with increasing sample area across most mid-to-high frequency bands, consistent with the edge effect discussed in Section 3, which is expected to be more pronounced for smaller samples.

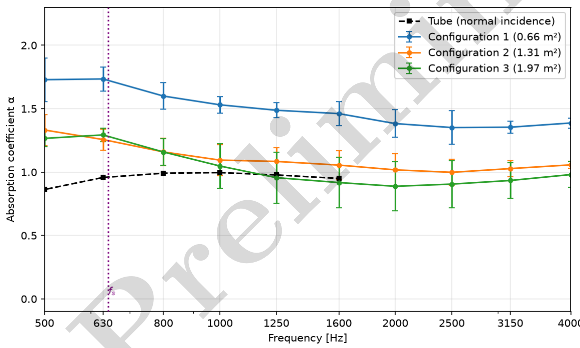

Figure 3: Comparison of $\alpha_{SSRR(f)}$ for the three configurations against the impedance tube.

5.2. Comparison with the impedance tube

The comparison between the absorption coefficients obtained with the SSRR method and those measured with the impedance tube was carried out using the normalized error criterion:

$$E_n(f) = \frac{|\alpha_{SSRR}(f) - \alpha_{tube}(f)|}{\sqrt{u_{SSRR}(f)^2 + u_{tube}(f)^2}} \quad (6)$$

with a compatibility threshold of $|E_n| < 1$ [30]. Above f_s, results depend markedly on the configuration tested. With 1 panel, no band is compatible, not even above f_s, where theory would predict favourable conditions. With 2 and 3 panels, compatibility is partial and closely comparable between the two: three of the four common bands above f_s are compatible in both cases (1000, 1250 and 1600 Hz), while 800 Hz, the band immediately above f_s, remains incompatible for both configurations. This suggests that the band closest to f_s is the least reliable for this comparison, and that a larger margin above the Schroeder frequency may be needed to ensure a robust match, regardless of sample area.

5.3. Consistency across measurement campaigns

An earlier measurement campaign, conducted with each panel configuration measured on a separate day rather than within a single session, showed the same overall pattern (1 panel always incompatible, 2 and 3 panels partially and comparably compatible) supporting the repeatability of these conclusions across different measurement protocols. Some band-specific differences were observed (3-panel configuration reaching full compatibility rather than 3/4), but given the day-to-day environmental variability inherent to that protocol, these are not treated as a substantive deviation from the main results.

6. Discussion

The results do not support a generic validation of the SSRR method, but a more precise one: above f_s, and provided the sample area is sufficiently large, α_{SSRR} and α_{tube} were found to be compatible. Testing three configurations was essential to this distinction, since a single configuration would not have revealed whether disagreement with the tube stemmed from a limitation of the method itself or simply from insufficient sample area.

Table 2: Absorption coefficients and normalized error E_n against the impedance tube

Hz	α_{tube}	$\alpha_{SSRR,C1}$	$E_{n,C1}$	$\alpha_{SSRR,C2}$	$E_{n,C2}$	$\alpha_{SSRR,C3}$	$E_{n,C3}$
800	0.991	1.600	5.58	1.159	1.49	1.158	1.53
1000	0.996	1.531	7.45	**1.094**	0.79	**1.048**	0.29
1250	0.978	1.488	7.61	**1.084**	0.96	**0.956**	0.11
1600	0.950	1.461	5.21	**1.055**	0.89	**0.918**	0.16

α_{SSRR} *values in bold satisfy the compatibility criterion* $|E_n| < 1$. *C1/C2/C3 = Configurations 1/2/3, as shown in Figure 1.*

The normal-incidence vs. random-incidence caveat. As discussed in Section 3, α_{SSRR} and α_{tube} are distinct physical quantities, only theoretically related, and numerical coincidence is not guaranteed. The impedance tube was used here as reference, unlike most SSRR validation studies, which compare against a FSRR [12], [13]. Compatibility above f_s should thus be read as numerical agreement within stated uncertainties, not conceptual equivalence, possibly aided by the convergence of normal- and random-incidence coefficients for highly absorptive materials, where little room remains for angular dependence to produce a different value.

Diffuse field and sample area as independent requirements. The persistent incompatibility of the 1-panel configuration, even above f_s, shows that the diffuse-field and sufficient-sample-area conditions are independent requirements: both necessary, neither sufficient alone. Even though the diffuse-field assumption holds above f_s, the edge effect remains dominant for small samples, inflating the measured α regardless. Only the 2- and 3-panel configurations, where both conditions hold, show the partial and comparable compatibility already reported in Section 5.2. This raises the practical question of how large an area is sufficient. Here, 1.3-2.0 m^2 (in a room of 8.96 m^3) proved enough, though not sufficient to resolve the band immediately above f_s, which warrants particular caution regardless of sample size. Together, these findings offer researchers a concrete starting point for designing similar setups.

References

[1] American Standards Association, "American Standard Acoustical Terminology," technical report Z24.1-1951, 1951.

[2] ISO, "Acoustics – Determination of Acoustic Properties in Impedance Tubes – Part 2," technical report ISO 10534-2:1998, 1998.

[3] ISO, "Acoustics: Measurement of sound absorption in a reverberation room," technical report ISO 354:2003, 2003.

[4] M. L. S. Vercammen, "On the revision of ISO 354, measurement of the sound absorption in the reverberation room," 2019.

[5] C. Scrosati and others, "Towards more reliable measurements of sound absorption coefficient in reverberation rooms: An Inter-Laboratory Test," *Appl. Acoust.*, vol. 165, 2020.

[6] H. Kuttruff and M. Vorländer, *Room Acoustics*. CRC Press, 2024.

[7] M. Nolan, "Estimation of angle-dependent absorption coefficients from spatially distributed in situ measurements," *J. Acoust. Soc. Am.*, vol. 147, no. 2, pp. EL119–EL124, 2020.

[8] L. Shtrepi and A. Prato, "Towards a sustainable approach for sound absorption assessment of building materials: Validation of small-scale reverberation room measurements," *Appl. Acoust.*, vol. 165, 2020.

[9] L. Ćurović, J. Murovec, A. Zeleznik, and J. Prezelj, "Estimation of sound absorption coefficient at modal frequencies using decay time measurements and eigenvalue model in a small room," *J. Low Freq. Noise Vib. Act. Control*, vol. 43, no. 4, pp. 1530–1544, 2024.

[10] J. R. Veen, J. Pan, and P. Saha, "Development of a Small Size Reverberation Room Standardized Test Procedure for Random Incidence Sound Absorption Testing," in *SAE 2005 Noise and Vibration Conf.*, 2005.

[11] SAE International, "Laboratory Measurement of Random Incidence Sound Absorption Tests Using a Small Reverberation Room," technical report J2883:2015, 2015.

[12] M. Kierzkowski, H. Law, and J. Cotterill, "Benefits of reduced-size reverberation room testing," in *Acoustics 2017*, 2017.

[13] R. del Rey, J. Alba, L. Bertó, and A. Gregori, "Small-sized reverberation chamber for the measurement of sound absorption," *Mater. Construcción*, vol. 67, no. 328, p. e139, 2017.

[14] M. R. Schroeder, "Frequency-Correlation Functions of Frequency Responses in Rooms," *J. Acoust. Soc. Am.*, vol. 34, no. 12, pp. 1819–1823, 1962.

[15] J. Y. Chung and D. A. Blaser, "Transfer function method of measuring in-duct acoustic properties. I. Theory," *J. Acoust. Soc. Am.*, vol. 68, no. 3, pp. 907–913, 1980.

[16] J. Y. Chung and D. A. Blaser, "Transfer function method of measuring in-duct acoustic properties. II. Experiment," *J. Acoust. Soc. Am.*, vol. 68, no. 3, pp. 914–921, 1980.

[17] E. Brandao, A. Lenzi, and S. Paul, "A Review of the In Situ Impedance and Sound Absorption Measurement Techniques," *Acta Acust. Acust.*, vol. 101, pp. 443–463, 2015.

[18] M. Garai, "Measurement of the sound-absorption coefficient in situ: The reflection method using periodic pseudo-random sequences of maximum length," *Appl. Acoust.*, vol. 39, no. 1, pp. 119–139, 1993.

[19] E. Mommertz, "Angle-dependent in-situ measurements of reflection coefficients using a subtraction technique," *Appl. Acoust.*, vol. 46, no. 3, pp. 251–263, 1995.

[20] J. F. Allard and Y. Champoux, "In Situ Two-Microphone Technique for the Measurement of the Acoustic Surface Impedance of Materials," *Noise Control Eng. J.*, vol. 32, no. 1, pp. 15–23, 1989.

[21] R. Lanoye, G. Vermeir, W. Lauriks, R. Kruse, and V. Mellert, "Measuring the free field acoustic impedance and absorption coefficient of sound absorbing materials with a combined particle velocity-pressure sensor," *J. Acoust. Soc. Am.*, vol. 119, no. 5, pp. 2826–2831, 2006.

[22] M. Tamura, "Spatial Fourier transform method of measuring reflection coefficients at oblique incidence. I," *J. Acoust. Soc. Am.*, vol. 88, no. 5, pp. 2259–2264, 1990.

[23] M. Tamura, J. F. Allard, and D. Lafarge, "Spatial Fourier-transform method for measuring reflection coefficients at oblique incidence. II," *J. Acoust. Soc. Am.*, vol. 97, no. 4, pp. 2255–2262, 1995.

[24] J. Hald, W. Song, K. Haddad, C.-H. Jeong, and A. Richard, "In-situ impedance and absorption coefficient measurements using a double-layer microphone array," *Appl. Acoust.*, vol. 143, pp. 74–83, 2019.

[25] S. Dupont, M. Sanalatii, M. Melon, O. Robin, A. Berry, and J.-C. Le Roux, "Measurement of the diffuse field sound absorption using a sound field synthesis method," *Acta Acust.*, vol. 7, p. 26, 2023.

[26] A. London, "The Determination of Reverberant Sound Absorption Coefficients from Acoustic Impedance Measurements," *J. Acoust. Soc. Am.*, vol. 22, no. 2, pp. 263–269, 1950.

[27] A. Cops, J. Vanhaecht, and K. Leppens, "Sound absorption in a reverberation room: Causes of discrepancies on measurement results," *Appl. Acoust.*, vol. 46, no. 3, pp. 215–232, 1995.

[28] W. C. Sabine, *Collected Papers on Acoustics*. Harvard University Press, 1922.

[29] ISO, "Acoustics – Measurement of room acoustic parameters – Part 2: Reverberation time in ordinary rooms," technical report ISO 3382-2:2008, 2008.

[30] ISO, "ISO/IEC 17043:2010 – Conformity assessment – General requirements for proficiency testing." 2010.